
Fairness Of AI Models in vector embedded Chest X-ray representations

Gebreyowhans H. Bahre^{1,2,4}, Hassan Hamidi^{1,4}, Andrew Sellergren⁵,
Leo Anthony Celi³, Francesco Calimeri², Laleh Seyyed-Kalantari^{1,4}

¹York University, ²University of Calabria, ³Massachusetts Institute of Technology, ⁴Vector Institute,
⁵Google
bahre@yorku.ca

Abstract

1 As deep learning models and datasets expand, the demand for computational re-
2 sources and memory storage intensifies; at the same time, data privacy concerns
3 hinder data and model sharing. Hence, accessibility of model training is signif-
4 icantly challenged. Vector embeddings, as compact representations of medical
5 images, offer a solution to the challenges of computational resource demands and
6 data privacy concerns in AI-based medical imaging. In this study we investigate
7 the suitability of vector embeddings as substitutes for original medical images in
8 disease prediction tasks, focusing on performance and fairness. Using datasets like
9 MIMIC-CXR and CheXpert, we find that vector embedding-based models gener-
10 ally improve disease detection performance and mitigate unfairness in diagnosis
11 rates. The reduced demographic signals in these embeddings may contribute to
12 fairer outcomes without compromising performance. Our findings suggest that
13 vector embeddings can enable more accessible and equitable medical computer
14 vision, particularly in low-resource settings.

15 1 Introduction

16 Artificial Intelligence (AI) can reduce healthcare costs, burnouts of staff, and geographical and social
17 disparities in care access. AI application in radiology has been showing promising results [Irvin et al.,
18 2019, Wang et al., 2017a, Ahluwalia et al., 2023, Rajpurkar et al., 2018].

19 However, building effective AI models is challenging, due to the need for extensive data [Akbarian
20 et al., 2023], high-performance computing, human expertise, and the risk of biases and unfair-
21 ness [Seyyed-Kalantari et al., 2021b,a, Nalla et al., 2024, Banerjee et al., 2023]. Here by unfairness
22 we mean consistent disparate outcomes of an AI model for a predictive task against some, typically
23 vulnerable, subpopulations.

24 Google recently released a CXR Foundation model⁶ that transforms chest radiograph images into
25 information-rich numerical vectors referred to as “vector embeddings” in an inference mode. So far,
26 Google has released the vector embedding representation of the MIMIC-CXR and CheXpert datasets
27 ^{2,4}. CXR Foundation models have been trained on a vast amount of natural and X-ray images.
28 Notably, using vector embeddings instead of original images reduces or even eliminates the need for
29 complex deep learning algorithm development, huge computation resources, and data storage, thus
30 paving the way to AI access equity. Such practice seems inevitable as models and training datasets
31 grow larger; however, whether vector embedding representations can effectively substitute for raw
32 medical images from both model performance and fairness perspectives is still an open question.

⁶<https://github.com/Google-Health/imaging-research/tree/master/cxr-foundation>

33 In this work, we evaluate fairness and performance of AI models trained on vector embedding vs
34 chest X-ray images in disease classification tasks. While there are concerns around AI race detection
35 from medical images [Gichoya et. al., 2022] and its impact on AI model fairness, we further explore
36 race and sex detection of AI models from vector embeddings vs medical images. The goal is to
37 verify whether vector embedding representations carry less demographic data (e.g., race or sex) than
38 medical images and explore its impact on model fairness. We compare models’ fairness in correct
39 disease diagnosis [Seyyed-Kalantari et al., 2021a] and underdiagnosis (unhealthy patient flagged as
40 healthy) [Seyyed-Kalantari et al., 2021b] in models that are trained on vector embedding and medical
41 images. We perform the analyses on large, publicly accessible vector embeddings of MIMIC-CXR
42 (MIMIC) and CheXpert (CXP) chest X-ray datasets, and a multi-source aggregation of both datasets,
43 referred to as *ALL*. Due to data availability, we use race, sex, and age as sensitive attributes for all
44 datasets, and insurance type as a proxy for socioeconomic status [Seyyed-Kalantari et al., 2021a] in
45 the MIMIC-CXR dataset. The main contribution of our work can be summarized as follows:

- 46 • Disease classification of AI model trained on vector embedding across 14 labels.
- 47 • Fairness analysis of the vector embedding-based disease detection model.
- 48 • Evaluating AI model race and sex detection from vector embedding vs medical images.
- 49 • Performing the aforementioned analyses on CheXpert, MIMIC-CXR, and their aggrega-
50 tion (*ALL*) datasets.

51 To the best of our knowledge, this work is the first benchmark of the above tasks to date. So far,
52 only disease classification of vector embedding-based model on five labels in 234 test samples of the
53 CheXpert has been reported [Sellergren et al., 2022].

54 **2 Related Work**

55 **2.1 Fairness and debiasing in medical imaging**

56 Recent studies showcased unfairness of AI models in disease diagnosis across various sensitive
57 attributes and underdiagnosis in chest X-ray disease classification for historically underserved popu-
58 lations [Seyyed-Kalantari et al., 2021a,b, Ahluwalia et al., 2023, Gichoya et al., 2023, Zhang et al.,
59 2022]. Underdiagnosis measured by False Positive Rate (FPR) on the No Finding label demonstrates
60 that the patient has a disease, but the classifiers detect the patient as healthy, potentially leading to
61 receiving no treatment. In the medical imaging domain, Larrazabal et al. [2020] evaluated unfairness
62 under gender imbalance training datasets. Limited efforts have been spent to address unfairness in
63 medical imaging, centred around benchmarking previous debiasing methods [Zhang et al., 2022]
64 and combining fine-tuning and pruning techniques [Marcinkevics et al., 2022]. MEDFAIR frame-
65 work Zong et al. [2022] assessed machine learning model fairness in medical imaging, highlighting
66 the prevalent bias in Empirical Risk Minimization (ERM) models across various modalities. Also
67 Zhang et al. [2021] evaluate the domain generalization techniques fairness and realize no method
68 outperforms ERM. Unfair AI can lead to escalating unfairness [Bohdal et al., 2023]. Fairness and
69 bias analysis in medical imaging needs domain-specific consideration of sensitive attributes [Heming
70 et al., 2023]. These techniques often reduce performance for privileged groups (e.g. White) rather
71 than improving it for non-privileged (e.g. Black) [Zhang et al., 2022, Marcinkevics et al., 2022].

72 **2.2 Short-cut learning from medical images**

73 AI models can predict human biological age [Lu et al., 2023], sex [Yang et al., 2021, Cao et al., 2021],
74 and race [Gichoya et. al., 2022], and even body mass index Abbasi Bavi et al. [2024] from medical
75 images. This is an undesired outcome as the AI model may use this data to further discriminate
76 against historically underserved populations. We hope that using vector embedding will degrade AI
77 demographic feature detection from medical images and mitigate unfairness, which needs further
78 investigation.

79 **2.3 Vector embedding representation**

80 Foundation models [Bommasani and et al., 2021, Yang et al., 2023], being large-scale deep AI
81 models trained on extensive datasets, can be applied across diverse tasks with minimal fine-tuning.

82 Google trained a CXR Foundation model and released vector embedding, the vector representation of
83 X-ray images in embedding space [Sellergren et al., 2022]. Vector embeddings condense intricate
84 information into concise vectors with 1376 floating-point representations for each chest X-ray image.
85 The model was initially trained on a large dataset of natural images, JFT-300M dataset [Sun et al.,
86 2017]. Subsequently, it was trained with supervised contrastive learning on noisy labels of normal/
87 abnormal over a dataset of 821, 544 chest radiographs, collected from India and the US [Sellergren
88 et al., 2022]. These datasets include five different hospitals in India, the ChestX-ray14 dataset (from
89 the National Institutes of Health(NIH)), and the US1 dataset (from a hospital system in Illinois, United
90 States). Note the datasets and disease labels in our study were not used to train CXR Foundation
91 models, and the images of our dataset are gathered from different geographical regions.

92 The disease prediction performance of vector embeddings has been presented for five labels [Seller-
93 gren et al., 2022] of the CheXpert dataset on a limited 234 samples. Glocker et al. [2022] conducted a
94 statistical bias analysis on the chest X-ray foundation model developed by Sellergren et al. [2022] on
95 the CheXpert dataset. Their findings revealed that the model embeds characteristics such as biological
96 sex and racial identity. Their disease detection performance shows around 5% degradation from Sell-
97 ergren et al. [2022], which might be due to different problem setups. Also, their fairness investigation
98 was based on fixed threshold selection leading to a demonstration of unfairness detection in CheXpert
99 vector embedding. Threshold selection significantly impacts fairness analysis [Seyyed-Kalantari
100 et al., 2022], and different values may be chosen based on needs. In the lack of specific preference for
101 the cost of false negative or positive prediction, a common approach focuses on threshold selection
102 based on maximizing the F1 score across all labels [Irvin et al., 2019, Seyyed-Kalantari et al., 2021a,
103 Rajpurkar et al., 2018] which was not the selection criteria for Glocker et al. [2022].

104

105 2.4 Transfer learning

106 While using vector embeddings might resemble transfer learning where a model is pre-trained and
107 its classification head is fine-tuned our approach goes beyond simple transfer learning. In the age
108 of foundation models, we explore the potential of generating enriched vector embeddings that can
109 substitute for original images, removing the need to continuously load, fine-tune, and deploy pre-
110 trained models. This novel approach of utilizing the embedding dataset significantly improves AI
111 accessibility in environments with limited resources, such as instrumentation and expertise, clearly
112 differentiating our method from traditional transfer learning.

113 3 Methods

114 3.1 Data

115 There are two publicly available Chest X-ray vector embedding datasets corresponding to the MIMIC-
116 CXR and Chexpert image datasets. We have done our analysis on these datasets and their aggregation
117 called ALL dataset. MIMIC-CXR⁵ dataset, collected from the Beth Israel Deaconess Medical
118 Center in Boston, MA, between 2011 and 2016 [Johnson et al., 2019] and its corresponding vector
119 embedding representation has been released by Google [Sellergren et al., 2023]⁶. The Chexpert⁷
120 dataset, which has gathered at the Stanford University Medical Center between October 2002 and July
121 2017 [Irvin et al., 2019], and its vector embedding representation has been released by Google⁸. Both
122 vector embedding datasets were derived from Google’s CXR-foundation model [Sellergren et al.,
123 2022]. Detailed information regarding the datasets, including distribution across patient subgroups
124 and diagnostic labels, can be found in Table A1 in supplementary materials and Table 1. We also
125 aggregated these two datasets to further explore the impact of using multi-source datasets.

126 We should note while the CXR foundation model could encode new datasets like chest-Xray14 [Wang
127 et al., 2017b], a data sharing agreement prevents us from sharing sensitive health data such as this
128 dataset with a third party (Google) to get the Vector Embedding representation. Also, since chest-

⁵<https://physionet.org/content/mimic-cxr-jpg/2.0.0/>

⁶<https://physionet.org/content/image-embeddings-mimic-cxr/1.0/>

⁷<https://stanfordaimi.azurewebsites.net/datasets/8cbd9ed4-2eb9-4565-affc-111cf4f7ebe2>

⁸<https://docs.google.com/forms/d/e/1FAIpQLSek0P-JSWSfonIiZJlZ7g0TbL0lugsDug0FUnMhS1zVzpeEK1g/viewform>

129 Xray14 has been used for training the Google foundation model with noisy labels of normal/abnormal,
 130 we should not conduct our analysis in this dataset to avoid data leakage. By doing our analysis on
 131 MIMIC-CXR and CheXpert, we have ensured none of our datasets has been used in training the
 132 Google X-ray foundation model.

133 3.2 Benchmarks

134 As baselines, we benchmark the following image-based models in MIMIC, CXP and ALL:

- 135 • Disease classification model trained on raw chest x-ray images from Seyyed-Kalantari et al.
 136 [2021a] and our in-house image-based model trained on ALL dataset.
- 137 • Fairness evaluation in performance (area under the ROC Curve (AUC)) correct disease
 138 diagnosis and underdiagnosis [Seyyed-Kalantari et al., 2021a,b] and our in-house image-
 139 based model trained on ALL.
- 140 • race detection from medical images [Gichoya et. al., 2022] for MIMIC-CXR and CheXpert
 141 and our in-house sex detection model from medical images across all datasets.

142 For vector embedding datasets of MIMIC, CXP and ALL, we benchmark the performance of our
 143 trained models on:

- 144 • The disease classification from chest x-ray vector embedding.
- 145 • Fairness evaluation in correct disease diagnosis and underdiagnosis.
- 146 • Race and sex detection of AI models from vector embedding.

147 3.3 Fairness evaluation

148 In this study, S denotes sensitive attributes, a criterion for eligibility for protection. In partic-
 149 ular, $S = \{S_{sex}, S_{age}, S_{race}\}$ for all datasets; and for MIMIC-CXR dataset also $S_{Insurance} \in$
 150 S . For every sensitive attribute, we consider a set of protected groups. Here, the protected
 151 groups are; $S_{sex} = \{male, female\}$, $S_{race} = \{White, Black, Hispanic, Other, Asian,$
 152 $AmericanIndian/Alaskanative\}$, $S_{age} = \{0 - 20, 20 - 40, 40 - 60, 60 - 80, 80-\}$, and
 153 $S_{insurance} = \{Medicare, Other, Medicaid\}$. Medicaid is a US governmental insurance for low-
 154 income families. Thus, we use insurance as a proxy for social economic status.

155 We evaluate the separation statistical fairness criteria, which, given the true label Y require orthogo-
 156 nality of predicted label \hat{Y} and S_i , $\hat{Y} \perp\!\!\!\perp S_i \mid Y$. Here, $Y, \hat{Y} \in \mathbb{R}^N$ and their elements $y_j, \hat{y}_j \in \{0,$
 157 $1\}$. Here, N is the number of disease labels. In MIMIC-CXR and CheXpert $N=14$.

158 Equality of odds [Hardt et al., 2016] notion of fairness satisfies separation criteria by equalizing
 159 the True Positive Rate (TPR) and FPR. We evaluate TPR disparities across disease labels [Seyyed-
 160 Kalantari et al., 2021a] and FPR differences across “No Finding” label [Seyyed-Kalantari et al.,
 161 2021b]. Similar to [Seyyed-Kalantari et al., 2021a], for binary S_i (e.g sex) the TPR disparity for the
 162 l th subpopulation within S_i , is given by

$$TPRDisp_{S_i;l} = TPR_{S_i;l} - TPR_{\neg S_i;l}. \quad (1)$$

163 Also, for the non-binary classification, similar to [Seyyed-Kalantari et al., 2021a], the TPR disparity
 164 for the l th subpopulation within S_i is given by:

$$TPRDisp_{S_i;l} = TPR_{S_i;l} - \text{Median}(\{TPR_{S_i;k}\}_{k=1}^l). \quad (2)$$

165 We calculate $TPRDisp_{S_i;l}$ per disease label y_j . For a given y_j , and S_i , the subgroup with maximum
 166 $TPRDisp_{S_i;l}$ is the most favorable as it has the largest disparity in favor. The most unfavorable
 167 groups revive the highest negative gap and $Gap_{i,j}$ are given by:

$$Gap_{i,j} = \max(\{TPRDisp_{S_i;k}\}_{k=1}^l) - \min(\{TPRDisp_{S_i;k}\}_{k=1}^l) \quad (3)$$

168 where, $Gap_{i,j}$ denotes the TPR disparity gap per disease label across subpopulations for a given
 169 S_i . We then calculate $\mathbb{E}[Gap_{i,j}]$, per S_i , across $\forall y_j$ and report it as the average $Gap_{i,j}$ for a given

170 sensitive attribute. Additionally, we zoom in “No Finding”(no disease diagnosed) label and evaluate
 171 the FPRs of this label as it measures the underdiagnosis rate similar to Seyyed-Kalantari et al. [2021b].
 172 A false positive of “No Finding” means the patient has a disease, but the classifier marks the patient
 173 as healthy.

174 3.4 Experiments

175 We conducted the following three major experiments.

176 **A) Disease classification with vector embedding-based model:** We evaluated three separate classi-
 177 fiers trained on vector embeddings of the MIMIC, CXP, and ALL datasets for disease classification
 178 and compared their outcomes to classifiers trained on chest X-ray images.

179 **B) Fairness evaluation of vector embedding-base model:** We assessed the fairness of the vector
 180 embedding-based model in correct disease diagnosis (TPR disparity) and flagging unhealthy patients
 181 healthy (underdiagnosis rate) in disease classification task.

182 **C) Race and sex detection using vector embedding:** We examine the ability of models trained on
 183 vector embeddings to detect race and sex.

184 3.5 Models

Label (Abbr.)	MIMIC(Img)	MIMIC(Emb)	CXP(Img)	CXP(Emb)	ALL(Img)	ALL(Emb)
Atelectasis (A)	0.837±0.001	0.809±0.001	0.717±0.001	0.908±0.000	0.891±0.004	0.887±0.001
Cardiomegaly (Cd)	0.828±0.002	0.805±0.001	0.855±0.003	0.902±0.000	0.887±0.004	0.884±0.000
Consolidation (Co)	0.844±0.001	0.826±0.002	0.734±0.004	0.906±0.000	0.938±0.003	0.936±0.000
Edema (Ed)	0.904±0.002	0.892±0.000	0.849±0.001	0.904±0.000	0.913±0.003	0.914±0.001
Enlarged Card (EC)	0.757±0.003	0.728±0.004	0.668±0.005	0.921±0.000	0.956±0.002	0.953±0.000
Fracture (Fr)	0.718±0.007	0.798±0.002	0.790±0.006	0.878±0.001	0.912±0.006	0.917±0.001
Lung Lesion (LL)	0.772±0.006	0.809±0.003	0.780±0.005	0.872±0.001	0.876±0.010	0.878±0.000
Lung Opacity (LO)	0.782±0.002	0.769±0.001	0.747±0.001	0.934±0.000	0.898±0.004	0.898±0.000
No Finding (NF)	0.868±0.001	0.867±0.000	0.885±0.001	0.955±0.000	0.911±0.005	0.912±0.001
Effusion (Ef)	0.933±0.001	0.909±0.000	0.885±0.001	0.904±0.000	0.916±0.004	0.911±0.000
Pleural Other (PO)	0.848±0.003	0.877±0.005	0.795±0.004	0.894±0.001	0.920±0.009	0.922±0.001
Pneumonia (Pa)	0.748±0.005	0.745±0.002	0.777±0.003	0.864±0.000	0.850±0.007	0.847±0.001
Pneumothorax (Px)	0.903±0.002	0.884±0.001	0.893±0.002	0.905±0.000	0.891±0.012	0.898±0.001
Sup. Dev. (SD)	0.927±0.001	0.928±0.000	0.898±0.001	0.942±0.001	0.929±0.006	0.941±0.000
Average (Avg)	0.834±0.001	0.832±0.000	0.805±0.001	0.906±0.000	0.906±0.006	0.907±0.000

Table 1: AUC (mean over 5 runs \pm 95% CI) for disease classification, trained on raw chest X-ray image-based model (Img) vs. our models trained on vector embeddings (Emb). The datasets are MIMIC-CXR (MIMIC), CheXpert (CXP), and their aggregation (ALL). The Img baseline of MIMIC and CXP are from Seyyed-Kalantari et al. [2021a]. Here, Sup. Dev. stands for support device.

185 All disease detection models (i.e., MIMIC-CXR, CXP, ALL(Emb), the classification head of
 186 ALL(Img)) and race and sex classification models have two hidden layers. Detailed configura-
 187 tions of all models are provided in Appendix B of supplementary materials. For ALL dataset
 188 image-based models, we utilized the DenseNet121, similar to other literatures [Irvin et al., 2019,
 189 Pooch et al., 2020, Rajpurkar et al., 2017, Seyyed-Kalantari et al., 2021b, Zhang et al., 2022]. The
 190 dataset was partitioned into training, validation, and testing sets according to a 80 – 10 – 10 split,
 191 ensuring no patient overlap. We report AUC and use TPR and FPR for fairness analysis.

192 4 Results

193 4.1 Disease classification performance using vector embedding

194 We present AUC for disease classification over 14 disease labels in MIMIC, CXP, and ALL datasets
 195 for both vector embedding-based model (Emb) and image-based model (Img). We used the results
 196 presented in Seyyed-Kalantari et al. [2021a] as the baseline for MIMIC and CXP, which itself
 197 compared its outcomes with other models [Tanno et al., 2019, Wang et al., 2020, Cohen et al., 2020,
 198 Allaouzi and Ben Ahmed, 2019] and achieved SOTA results. For ALL datasets, we trained an
 199 in-house image-based model. Notably, ALL datasets in Seyyed-Kalantari et al. [2021a] also include

200 the Chest X-ray 14 dataset, which has been used in training of Google CXR Foundation model
 201 [Sellergren et al., 2022]. Therefore, we trained both image-based and vector-embedding models for
 202 ALL datasets, including only CXP and MIMIC datasets.

203 Table 1 shows the AUCs across labels. Our vector embedding-based models perform better on average
 204 across all labels in disease classification tasks for CXP and ALL datasets, particularly showing a
 205 notable 0.1 AUC boost for CXP. In MIMIC, the image-based model’s AUC is negligibly 0.002 higher.
 206 The Google CXR Foundation model paper [Sellergren et al., 2022] provides vector embedding-based
 207 results for five CXP labels, only for 234 hand-labeled test images, which are not publicly available.
 208 However, our test set covered 14 labels on a large test set of 19, 471 images for CheXpert, 21, 591 for
 209 MIMIC-CXR, and 41, 062 for ALL datasets. Overall, our AUCs are better or similar for all those five
 210 labels [Sellergren et al., 2022], except for Effusion, where ours is 0.03 lower. We report the mean and
 211 95% confidence interval achieved from different random seed. Training was conducted using 20 CPU
 212 cores, 32GB RAM, and an NVIDIA RTX 6000 GPU, completing in 7,5, and 12 minutes for MIMIC,
 213 CXP, and ALL vector embedding datasets, respectively. In contrast, training the ALL image-based
 214 model typically takes about 10 hours. In summary, vector embeddings allow to accomplish the task
 215 faster with much lower computational power, and lead to better performance compared to medical
 216 images based models [Seyyed-Kalantari et al., 2021b, Tanno et al., 2019, Cohen et al., 2020, Wang
 217 et al., 2020, Allaouzi and Ben Ahmed, 2019].

218 **4.2 Fairness Results**

219 **4.2.1 TPR Disparities**

220 We have evaluated TPR disparities using Eq. 1 for sex and Eq. 2 for the remaining sensitive attributes.
 221 Here, positive and negative disparities reflect biases favouring or unfavouring particular subgroups.
 222 Here, the most favorable groups have the largest frequency of positive gaps across 13 disease labels,
 223 and the most unfavorable has the largest frequency of negative gaps. Figure 1 shows the distribution
 224 of race TPR disparities with 95% CI, sorted by Gap_j for a model trained on the ALL dataset. Here,
 225 $\mathbb{E}[Gap_{race,j}], \forall j$, is 0.214, “Support Devices(SD)” has the least gap 0.037 and “Pneumonia(Pn)” has
 226 the most 0.376. “Black” patients constantly receive negative TPR disparities in 13/13 disease labels.
 227 We refer to them as the most unfavorable group, while patients with “Other” races reviving the most
 228 frequently positive TPR disparities 13/13 are referred to as the most favorable groups. We plot TPR
 229 disparities for remaining sensitive attributes and datasets in Figures C1 to C9 of supplementary
 230 materials. We summarized all TPR disparity average gaps across all labels, the disease with the
 231 lowest and highest gap, and the most favorable and unfavorable subpopulation in Table 2. Ideally, we
 232 would have negligible TPR disparities across all subgroups, within each label (“No Finding” label
 has been excluded to focus in disease diagnosis.).

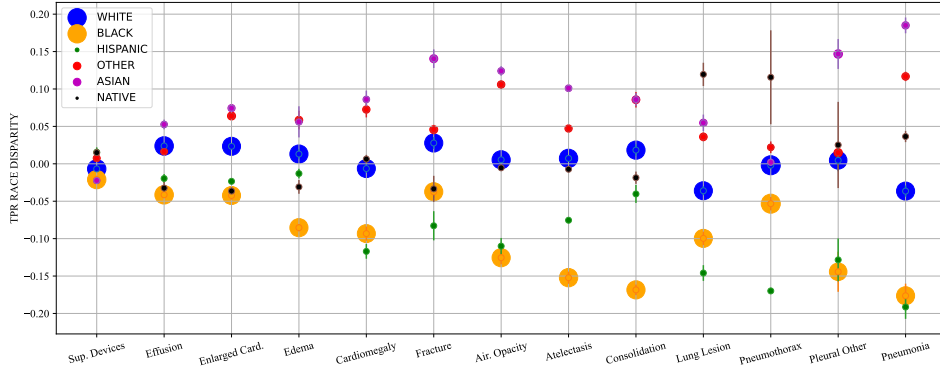


Figure 1: TPR race disparities (mean over 5 run \pm 95% CI indicated by arrows) of ALL dataset (y-axis) across disease labels (x-axis). The scatter plot size corresponds to the subgroup sizes per label. Here, positive TPR disparities are favourable, while negative disparities are unfavourable. Notably, Black patients are the unfavourable group for all 13 disease labels, and patients of other racial groups are the most favourable subgroup. For a particular disease, the lower the distance, the fairer the model. We summarized these outcome in Table 2.

Attribute	Dataset	Average Gap	Cross-Label Gap		Unfavorable	Favorable
			Lowest	Highest		
Sex	ALL(Emb)	0.042	Fr:0.007	LL:0.114	Female(10/13)	Male(10/13)
	ALL(Img)	0.069	PE:0.024	Ed:0.139	Female(12/13)	Male(12/13)
	MIMIC(Emb)	0.071	PE:0.008	LL:0.217	Female(11/13)	Male(11/13)
	MIMIC(Img)	0.072	Ed:0.011	EC:0.151	Female(10/13)	Male(10/13)
	CXP(Emb)	0.024	Pn:0.000	Ed:0.049	Female(9/13)	Male(9/13)
	CXP(Img)	0.062	ED:0.000	Co:0.139	Female(7/13)	Male(7/13)
Age	ALL(Emb)	0.103	PE:0.029	Px:0.266	20-40(11/13)	60-80(12/13)
	ALL(Img)	0.122	FR:0.054	EC:0.194	20-40(10/13)	60-80(13/13)
	MIMIC(Emb)	0.190	SD:0.059	PE:0.405	80-(9/13)	60-80(9/13)
	MIMIC(Img)	0.245	SD:0.091	Cd:0.440	0-20, 20-40(7/13)	60-80(10/13)
	CXP(Emb)	0.114	Co:0.037	Px:0.251	0-20,20-40(10/13)	60-80(13/13)
	CXP(Img)	0.270	SD:0.084	NF:0.604	0-20, 20-40, 80-(7/13)	40-60(8/13)
Race	ALL(Emb)	0.214	SD:0.037	Pn:0.376	Black(13/13)	Other(13/13)
	ALL(Img)	0.183	EC:0.113	PX:0.316	Black(13/13)	Asian(13/13)
	MIMIC(Emb)	0.280	Cd:0.109	Px:0.663	Black,Asian(9/13)	White(10/13)
	MIMIC(Img)	0.226	NF:0.119	Pa:0.440	Hispanic(9/13)	White(9/13)
	CXP(Emb)	0.100	LL:0.035	Fr:0.186	Black,Native(12/13)	White,Asian(10/13)
	CXP(Img)	0.119	Fr:0.055	At:0.215	Native(9/13)	Other(7/13)
Insurance	MIMIC(Emb)	0.008	At:0.0005	Co:0.029	Medicare(8/13)	Other(9/13)
	MIMIC(Img)	0.100	SD:0.021	PO:0.190	Medicaid(10/13)	Other(10/13)

Table 2: Summary of TPR disparities across sensitive attributes for image-based (Img) [Seyyed-Kalantari et al., 2021a] versus vector embedding-based (Emb) models. We calculate the $\mathbb{E}[Gap_{i,j}], \forall i, \forall j$, as listed in the Average Gap column. A smaller average gap indicates a fairer model in disease diagnosis. The lowest and highest gaps per attribute/dataset, along with their values, are shown (full disease names in Table 1). The most Unfavorable/favorable subgroups have also been shown. Only MIMIC has insurance data.

234 In cases of minimal average gap, our model shows improved fairness regarding TPR disparity. As
235 before, compare fairness between models trained on vector embeddings (Emb) and images (Img),
236 with baseline results from Seyyed-Kalantari et al. [2021a], except for ALL. Vector embedding
237 models consistently show a lower average gap for sex, age, and insurance attributes across MIMIC,
238 CXP, and ALL datasets, indicating fairer outcomes compared to image models. However, for race
239 in ALL and MIMIC, vector embeddings have a higher gap. The most and least favored subgroups
240 generally remain unchanged between vector embedding and image models.

241 4.2.2 Underdiagnosis

242 For CXP, Fig. 2 shows the underdiagnosis rate using vector embeddings vs medical images across
243 subgroups of sex, age, and race and the patients’ intersection with two/three underserved groups. We
244 report the baseline results from Seyyed-Kalantari et al. [2021b], shown in gray color in Fig. 2. We
245 exclude groups with fewer than 10 patients with FPR from the plot to avoid conclusions based on
246 small subsets. No three-group intersections meet this criterion, so we do not provide such plots.

247 Vector embedding reduces the underdiagnosis rate and narrows the fairness gap between the maximum
248 and minimum rates per sensitive attribute, improving fairness in the max-min gap of underdiagnosis.
249 We also evaluate the underdiagnosis rate for the MIMIC-CXR and ALL datasets. Table D1 in the
250 supplementary materials summarizes underdiagnosis rate fairness, with detailed findings in Figures
251 D1 and D2.

252 For the MIMIC-CXR dataset, vector embedding models reduced underdiagnosis rates and max-min
253 gaps across all subgroups compared to image-based models. In ALL data, both models show similar
254 underdiagnosis rates and max-min gaps (Fig D1). The image model has a slightly lower FPR for
255 three age subgroups, but the difference is minimal, with the max-min gap only 0.002 higher for vector
256 embedding.

257 4.3 Sex and race detection using vector embedding

258 We aim to determine if models can learn sensitive features like race and sex when using vector
259 embeddings. Lower detection of these features is preferred, as using demographic data may lead to
260 unfairness. Table C1 in the supplementary materials shows the AUC for sex and race detection in

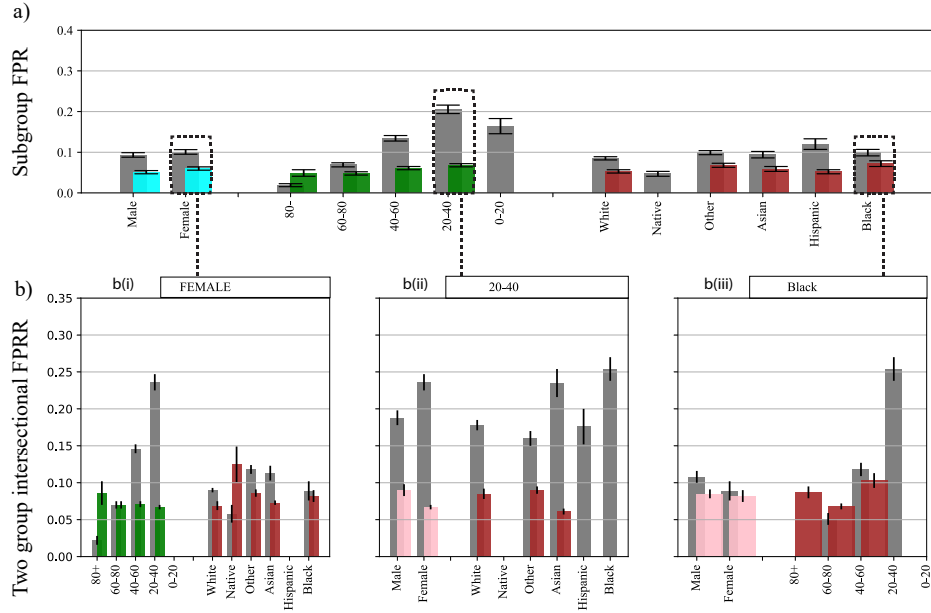


Figure 2: Exploration of underdiagnosis rates. (a) rates across sex, age, and race subgroups in CheXpert. (b), Two group intersection underdiagnosis rates for (b(i)) female, (b(ii)), 20-40, and (b(iii)) Black patients amidst all other subgroups. Subgroups with fewer than ten FPR occurrences are excluded. The gray bar represents the image-based model from Seyyed-Kalantari et al. [2021b]. Here, using vector embeddings reduced the max-min FPR gap and overall underdiagnosis rate, leading to more fairness. Most underdiagnosis groups and max-min gap are presented in Table D1 of supplementary materials.

261 different settings. While vector embeddings still carry these signals, detecting race and sex is easier
 262 in images, as shown by the lower AUC in vector embeddings.

263 5 Discussion

264 5.1 Vector embeddings: reliable substitute for X-ray images

265 **Disease classification performance:** On average, vector embedding-based disease classifiers
 266 outperform image-based models across all labels in CheXpert and multi-source ALL datasets (see
 267 Table 1). In MIMIC-CXR, the image-based model only slightly outperforms by 0.002, which is
 268 negligible compared to the computational savings. Thus, vector embeddings are a reliable substitute
 269 for raw images for AI model training.

270 **Fairness:** For fairness, we compared TPR disparity, underdiagnosis rate, and max-min gap in
 271 underdiagnosis. Vector embeddings generally improve TPR disparity across all labels in most of
 272 the dataset-sensitive attribute setup pairs, reducing the gap in 8 of 10 sensitive attribute setups (see
 273 Table 2). Similarly, vector embeddings often reduce both the underdiagnosis rate and the max-min
 274 gap compared to image-based models (Table D1), doing so in 7 out of 10 dataset-attribute pairs.
 275 For cases where the gap isn't smaller, the difference is minimal, ranging from 0.002 to 0.007. This
 276 outcome indicates greater fairness in the vector embedding model compared to the image-based
 277 model. We also examined multi-source data, where both model types perform similarly in disease
 278 detection, showing minimal max-min gaps in underdiagnosis and often small average diagnosis gaps.
 279 This suggests that large multi-source datasets can reduce disparities, aligning image-based models
 280 more closely with the representations learned by foundation models.

281 **Vulnerable groups:** The vector embedding-based model does not alter vulnerable subgroups,
 282 with female, younger, and Black patients still being the most underdiagnosed (see Tables 2 and Table
 283 D1 in supplementary materials). Additionally, TPR disparity shifts from Medicaid to Medicare when

284 using vector embeddings. This group represents retired patients, typically of lower socioeconomic
285 status, with Medicaid remaining the most underdiagnosed. Groups with multiple vulnerable traits,
286 such as Black females, face higher underdiagnosis rates than white females, indicating amplified bias.
287 These findings align with previously identified vulnerable groups in healthcare [Abdelmalek et al.,
288 2023] and medical imaging [Seyyed-Kalantari et al., 2021a,b], reflecting existing societal biases.

289 **Diversity and the size of data:** The image-based and vector embedding-based models demon-
290 strate similar performance in disease detection and underdiagnosis rates across various datasets
291 and attributes. The multi-source dataset is notably larger and more diverse than individual datasets.
292 These features may help achieve performance closer to the vector embedding dataset, originally
293 derived from a foundation model trained on large, diverse data. Similarly, vector embedding yields
294 greater performance improvements in the CheXpert dataset compared to the MIMIC-CXR dataset,
295 as CheXpert was initially smaller. These findings suggest that vector embedding may offer greater
296 benefits in fairness and performance with smaller, less diverse original datasets. As data size increases,
297 the advantages of using vector embedding or image-based models for improved performance and
298 fairness diminish. Nonetheless, vector embedding still provides the benefit of faster training with
299 lower computational resources.

300 **Generalizability:** Across datasets, vector embedding-based models consistently improved model
301 fairness compared to image-based models. However, the vulnerable subgroups remained unchanged
302 with vector embedding. It’s important to note that fairness analysis outcomes on binary predictions
303 can vary significantly with different thresholds. In this work, similar to prior studies [Seyyed-Kalantari
304 et al., 2021a,b, Rajpurkar et al., 2017], we use the threshold that maximizes the F1 score across all
305 labels, treating precision and recall equally. However, one can set the threshold to achieve a fixed
306 FPR for disease classification [Glocker et al., 2022]. The choice of threshold depends on the specific
307 problem and the associated costs of precision and recall in the downstream task.

308 5.2 The fairer, the blinder to demographic features

309 Our findings suggest that demographic features such race and sex persists in vector embedding
310 but the race and sex detection performance is less than image-based model. Concurrently, vector
311 embeddings reduce unfairness in disease diagnosis and underdiagnosis rates compared to image-
312 based models. Digging into numbers among three datasets, CXP has more fairness (less average gap)
313 in correct disease diagnosis (See Table 2) and less max-min gap in underdiagnosis rate analysis
314 (See Table D1 of supplementary materials. This co-occurs with often less sex and race detection
315 performance (See Table C1 of supplementary materials). In particular, for the CheXpert dataset, we
316 observe the race signal dropped more in vector embedding, co-occurring with higher performance in
317 disease detection (See Table 1), and less unfairness (See Table 2). Such observation amplifies the
318 importance of learning representation with less sensitive signals to mitigate unfairness.

319 5.3 Vector embedding: AI equity and lower environmental damage

320 Our work shows that vector embeddings enhance AI efficiency and fairness while reducing memory
321 and GPU usage, leading to lower carbon emissions and environmental impact. This approach makes
322 AI more accessible to those with limited computational resources or expertise. Releasing and using
323 vector embedding datasets as image substitutes can promote global AI equity. As AI models grow
324 and become constrained to high-tech companies, vector embeddings offer a viable alternative for
325 those lacking advanced computing infrastructure.

326 6 Limitations and Future Work

327 Considering the potential benefits showcased by the vector embedding dataset, we propose the
328 expansion of producing vector embedding versions of diverse datasets. This expansion will broaden
329 our fairness analysis to include a wider range of vector embedding datasets, diverse demographic
330 profiles, and various analytical techniques. Our work relies on two only available vector embedding
331 datasets, MIMIC-CXR and CheXpert, along with their aggregations. In addition, the backbone
332 CXR foundation model [Sellergren et al., 2022] that generated the vector embeddings is trained on
333 data collected from limited resources in the USA and India, raising concerns about data shift and

334 drift. Using a larger and diversified dataset for these foundation models potentially leads to a more
335 generalizable representation of learning. We plan to develop a fair vector embedding representation
336 for future work that leads to fairer outcomes. Considering recent progress in large language models
337 (LLMs), We also plan to consider multi-modality in analyzing the vector embedding or learning
338 fair vector embeddings. In doing so, the fairness of applied LLMs needs to be considered so as
339 not to enforce extra biases [Tian et al., 2023]. Following the hints from this research, locating
340 demographic signals [Salvado et al., 2024] and disentangling or mitigating demographic signals from
341 vector embedding representation seems to be a plausible path to reach our goal. We will also generate
342 vector embedding representations for diverse public medical image datasets and release them for the
343 public community’s use.

344 7 Conclusion

345 We examined the fairness and performance of the disease classification AI model using vector em-
346 bedding datasets and image-based datasets. Overall, the vector embedding-based model outperforms
347 or has a negligible drop in disease classification performance and improved fairness compared to the
348 image-based model, suggesting vector embeddings are a proper substitute for medical images in AI
349 model training. We observed large and multi-source datasets demonstrate less difference in fairness
350 and performance between models based on vector embedding and image. Additionally, there are
351 fewer demographic features such as race and sex information in vector embedding vs images, which
352 may guide researchers to look for ways to learn representation with fewer demographic features to
353 reach better fairness. We should also note training a model for the classification of vector embedding
354 datasets requires less computational power and specialized knowledge while promoting privacy and
355 equity in AI access and reducing negative computational environmental impact.

356 8 Acknowledgments

357 This work has received partial support from the PNRR project FAIR - Future AI Research
358 (PE00000013), Spoke 9 - Green-aware AI, under the NRRP MUR program funded by NextGenera-
359 tionEU(to Gebreyowhans H. Bahre). We sincerely thank the Natural Sciences and Engineering
360 Research Council of Canada (NSERC) for the Discovery Grant (to Dr. Laleh Seyyed-Kalantari) and
361 the Connected Minds CFREF (to Dr. Seyyed-Kalantari). The authors also express their gratitude to
362 the Vector Institute for providing high-performance computing platforms.

363 References

- 364 E. Abbasi Bavil, M. Ahluwalia, L. Seyyed-Kalantari, B. Fine, and M. Abdalla. Body mass index
365 prediction from chest radiographs and associated performance gaps in chest radiograph abnormality
366 prediction. In *CAR 2024 Annual Scientific Meeting (ASM)*, Montréal, Canada, 2024.
- 367 Fred M. Abdelmalek, Federico Angriman, Julie Moore, Kuan Liu, Lisa Burry, Laleh Seyyed-
368 Kalantari, Sangeeta Mehta, Judy Gichoya, Leo Anthony Celi, George Tomlinson, Michael Fralick,
369 and Christopher J. Yarnell. Association between patient race and ethnicity and use of invasive
370 ventilation in the united states. *Annals of the American Thoracic Society*, 21(2):Specific Page
371 Range, Nov 2023. doi: SpecificDOI. Impact Factor: 8.3.
- 372 M. Ahluwalia, M. Abdalla, J. Sanayei, L. S. Kalantari, M. Hussain, A. Ali, and B. Fine. The
373 subgroup imperative: Chest x-ray classifier generalization gaps in patient, setting, and pathology
374 subgroups. *Radiology: Artificial Intelligence*, 5(2):e230020, 2023. doi: 10.1148/ryai.230020.
375 URL <https://doi.org/10.1148/ryai.230020>.
- 376 S. Akbarian, L. Seyyed-Kalantari, F. Khalvati, and E. Dolatabadi. Evaluating knowledge transfer
377 in the neural network for medical images. *IEEE Access*, 11:85812–85821, 2023. doi: 10.1109/
378 ACCESS.2023.3283216.
- 379 Imen Allaouzi and Mohamed Ben Ahmed. A novel approach for multi-label chest x-ray classification
380 of common thorax diseases. *IEEE Access*, 7:64279–64288, 2019. doi: 10.1109/ACCESS.2019.
381 2916849.

- 382 I. Banerjee, K. Bhattacharjee, J. L. Burns, H. Trivedi, S. Purkayastha, L. S. Kalantari, B. N. Patel,
383 R. Shiradkar, and J. Gichoya. “shortcuts” causing bias in radiology artificial intelligence: Causes,
384 evaluation, and mitigation. *Journal of the American College of Radiology*, 20(9), September 2023.
- 385 Ondrej Bohdal, Timothy Hospedales, Philip HS Torr, and Fazl Barez. Fairness in ai and its long-term
386 implications on society. *arXiv preprint*, arXiv:2304.09826, 2023. URL [https://arxiv.org/
387 abs/2304.09826](https://arxiv.org/abs/2304.09826).
- 388 Rishi Bommasani and et al. On the opportunities and risks of foundation models. *arXiv preprint*,
389 2021. URL <https://arxiv.org/abs/2108.07258>.
- 390 Y. Cao, Y. Ma, D.N. Vieira, et al. A potential method for sex estimation of human skeletons using
391 deep learning and three-dimensional surface scanning. *International Journal of Legal Medicine*,
392 135:2409–2421, 2021. doi: 10.1007/s00414-021-02675-z. URL [https://doi.org/10.1007/
s00414-021-02675-z](https://doi.org/10.1007/
393 s00414-021-02675-z).
- 394 Joseph Paul Cohen, Muhammad Hashir, Rupert Brooks, and Hannah Bertrand. On the limits of
395 cross-domain generalization in automated x-ray prediction. *arXiv preprint arXiv:2002.02497*,
396 2020.
- 397 Judy Wawira Gichoya, Kaesha Thomas, Leo Anthony Celi, Nabile Safdar, Imon Banerjee, John D
398 Banja, Laleh Seyyed-Kalantari, Hari Trivedi, and Saptarshi Purkayastha. Ai pitfalls and what
399 not to do: mitigating bias in ai. *British Journal of Radiology*, 96(1150), October 2023. doi:
400 10.1259/bjr.20230023. URL <https://doi.org/10.1259/bjr.20230023>.
- 401 Judy Wawira Gichoya et. al. Ai recognition of patient race in medical imaging: a modelling study.
402 *The Lancet. Digital health*, 4:e406–e414, 2022. doi: 10.1016/S2589-7500(22)00076-2.
- 403 Ben Glocker, Charles Jones, Melanie Bernhardt, and Stefan Winzeck. Risk of bias in chest x-ray
404 foundation models. *arXiv preprint*, 2022. URL <https://arxiv.org/abs/2209.02965>.
- 405 Moritz Hardt, Eric Price, and Nathan Srebro. Equality of opportunity in supervised learning. *arXiv
406 preprint arXiv:1610.02413*, 2016. <https://arxiv.org/abs/1610.02413>.
- 407 Carolina A. M. Heming, Mohamed Abdalla, Monish Ahluwalia, Linglin Zhang, Hari Trivedi, MinJae
408 Woo, Benjamin Fine, Judy Wawira Gichoya, Leo Anthony Celi, and Laleh Seyyed-Kalantari.
409 Benchmarking bias: Expanding clinical ai model card to incorporate bias reporting of social and
410 non-social factors, 2023.
- 411 Jeremy A. Irvin, Pranav Rajpurkar, Michael Ko, Yifan Yu, Silviana Ciurea-Ilcus, Chris Chute, Henrik
412 Marklund, Behzad Haghgoo, Robyn L. Ball, Katie S. Shpanskaya, Jayne Seekins, David Andrew
413 Mong, Safwan S. Halabi, Jesse K. Sandberg, Ricky Jones, David B. Larson, Curtis Langlotz,
414 Bhavik N. Patel, Matthew P. Lungren, and Andrew Ng. Chexpert: A large chest radiograph
415 dataset with uncertainty labels and expert comparison. *Proceedings of the AAAI Conference
416 on Artificial Intelligence*, 33(01):590–597, July 2019. doi: 10.1609/aaai.v33i01.3301590. URL
417 <https://doi.org/10.1609/aaai.v33i01.3301590>.
- 418 Alistair E. W. Johnson, Tom J. Pollard, Nathaniel R. Greenbaum, Matthew P. Lungren, Chih ying
419 Deng, Yifan Peng, Zhiyong Lu, Roger G. Mark, Seth J. Berkowitz, and Steven Horng. Mimic-cxr-
420 jpg, a large publicly available database of labeled chest radiographs. *Computer Vision and Pattern
421 Recognition*, 2019.
- 422 Agostina J. Larrazabal, Nicolás Nieto, Victoria Peterson, Diego H. Milone, and Enzo Ferrante.
423 Gender imbalance in medical imaging datasets produces biased classifiers for computer-aided
424 diagnosis. *Proceedings of the National Academy of Sciences*, 117(23):12592–12594, 2020.
- 425 T. Lu, Yr. Diao, Xe. Tang, et al. Deep learning enables automatic adult age estimation based
426 on ct reconstruction images of the costal cartilage. *Eur Radiol*, 33:7519–7529, 2023. doi:
427 10.1007/s00330-023-09761-3. URL <https://doi.org/10.1007/s00330-023-09761-3>.
- 428 Ricards Marcinkevics, Ece Ozkan, and Julia E. Vogt. Debiasing deep chest x-ray classifiers using
429 intra-and post-processing methods. In *Machine Learning for Healthcare Conference*, pages
430 504–536. PMLR, 2022.

- 431 Vineela Nalla, Seyedamin Pouriyeh, Reza M. Parizi, Hari Trivedi, Quan Z. Sheng, Inchan Hwang,
432 Laleh Seyyed-Kalantari, and MinJae Woo. Deep learning for computer-aided abnormalities
433 classification in digital mammogram: A data-centric perspective. *Current Problems in Diagnostic*
434 *Radiology*, 53(1):1–10, January 2024. doi: 10.1067/j.cpradiol.2023.10.001. URL <https://doi.org/10.1067/j.cpradiol.2023.10.001>.
- 436 Eduardo H P Pooch, Pedro Ballester, and Rodrigo C Barros. Can we trust deep learning based
437 diagnosis? the impact of domain shift in chest radiograph classification. In *Thoracic Image*
438 *Analysis. TIA 2020*, volume 12502, Cham, 2020. Springer. doi: 10.1007/978-3-030-62469-9_7.
439 URL https://doi.org/10.1007/978-3-030-62469-9_7.
- 440 Pranav Rajpurkar, Jeremy Irvin, Kaylie Zhu, Brandon Yang, Hershel Mehta, Tony Duan, Daisy
441 Ding, Aarti Bagul, Curtis Langlotz, Katie Shpanskaya, Matthew P Lungren, and Andrew Y Ng.
442 Chexnet: Radiologist-level pneumonia detection on chest x-rays with deep learning. *arXiv preprint*
443 *arXiv:1711.05225*, 2017.
- 444 Pranav Rajpurkar, Jeremy Irvin, Robyn L Ball, Kaylie Zhu, Brandon Yang, Harsh Mehta, Tony Duan,
445 Daisy Ding, Aarti Bagul, Curtis P Langlotz, et al. Deep learning for chest radiograph diagnosis: A
446 retrospective comparison of the chexnext algorithm to practicing radiologists. *PLoS Med*, 15(11):
447 e1002686, Nov 2018. doi: 10.1371/journal.pmed.1002686.
- 448 Olivier Salvado, Salamata Konate, Rodrigo Santa Cruz, Andrew Bradley, Judy Wawira Gichoya,
449 Laleh Seyyed-Kalantari, Brandon Price, Clinton Fookes, and Leo Lebrat. Localisation of racial
450 information in chest x-ray for deep learning diagnosis. In *Proceedings of the International*
451 *Symposium on Biomedical Imaging (ISBI)*, Athens, Greece, 2024.
- 452 A. Sellergren, A. Kiraly, T. Pollard, W. Weng, Y. Liu, A. Uddin, and C. Chen. Generalized image
453 embeddings for the mimic chest x-ray dataset (version 1.0). *PhysioNet*, 2023. <https://doi.org/10.13026/pxc2-vx69>.
- 455 A. B. Sellergren, C. Chen, Z. Nabulsi, Y. Li, A. Maschinot, A. Sarna, J. Huang, C. Lau, S. R.
456 Kalidindi, M. Etemadi, F. Garcia-Vicente, D. Melnick, Y. Liu, K. Eswaran, D. Tse, N. Beladia,
457 D. Krishnan, and S. Shetty. Simplified transfer learning for chest radiography models using less
458 data. *Radiology*, 305(2):454–465, 2022. doi: 10.1148/radiol.212482.
- 459 Laleh Seyyed-Kalantari, Guanxiong Liu, Matthew B. A. McDermott, and Marzyeh Ghassemi.
460 Chexclusion: Fairness gaps in deep chest x-ray classifiers. *Pacific Symposium on Biocomputing*,
461 26:232–243, 2021a.
- 462 Laleh Seyyed-Kalantari, Haoran Zhang, Matthew BA McDermott, Irene Y. Chen, and Marzyeh
463 Ghassemi. Underdiagnosis bias of artificial intelligence algorithms applied to chest radiographs in
464 under-served patient populations. *Nature Medicine*, 27(12):2176–2182, 2021b.
- 465 Laleh Seyyed-Kalantari, Haoran Zhang, Matthew B.A. McDermott, Irene Y. Chen, and Marzyeh
466 Ghassemi. Reply to: ‘potential sources of dataset bias complicate investigation of underdiagnosis
467 by machine learning algorithms’ and ‘confounding factors need to be accounted for in assessing
468 bias by machine learning algorithms’. *Nature Medicine*, 28:1161–1162, 2022. doi: 10.1038/
469 s41591-022-01854-8. URL <https://www.nature.com/articles/s41591-022-01854-8>.
- 470 Chen Sun, Abhinav Shrivastava, Saurabh Singh, and Abhinav Gupta. Revisiting unreasonable
471 effectiveness of data in deep learning era, 2017.
- 472 Ryosuke Tanno, Ardavan Saeedi, Swami Sankaranarayanan, Daniel C Alexander, and Nathan
473 Silberman. Learning from noisy labels by regularized estimation of annotator confusion. *arXiv*
474 *preprint arXiv:1902.03680*, 2019.
- 475 Jacob-Junqi Tian, D. Emerson, Deval Pandya, Laleh Seyyed-Kalantari, and Faiza Khattak. Effi-
476 cient evaluation of bias in large language models through prompt tuning. In *Proceedings of the*
477 *Conference on Neural Information Processing Systems*, 2023. URL <https://openreview.net/forum?id=v1WL011gp8>.
- 479 Xiaogang Wang, Zhen Xu, Dongkuan Yang, Lai Tam, Holger Roth, and Dong Xu. Learning image
480 labels on-the-fly for training robust classification models. *arXiv preprint arXiv:2009.10325*, 2020.

- 481 Xiaosong Wang, Yifan Peng, Le Lu, Zhiyong Lu, Mohammadhadi Bagheri, and Ronald M. Summers.
482 ChestX-ray8: Hospital-scale chest x-ray database and benchmarks on weakly-supervised classifica-
483 tion and localization of common thorax diseases. *Proceedings of the IEEE Conference on Computer*
484 *Vision and Pattern Recognition*, 1(2):2097–2106, July 2017a. doi: 10.1109/CVPR.2017.845. URL
485 <https://doi.org/10.1109/CVPR.2017.845>.
- 486 Xiaosong Wang, Yifan Peng, Le Lu, Zhiyong Lu, Mohammadhadi Bagheri, and Ronald M.
487 Summers. ChestX-ray8: Hospital-Scale Chest X-Ray Database and Benchmarks on
488 Weakly-Supervised Classification and Localization of Common Thorax Diseases. In *Com-*
489 *puter Vision and Pattern Recognition (CVPR) 2017*, pages 2097–2106. IEEE, 2017b.
490 URL [http://openaccess.thecvf.com/content_cvpr_2017/html/Wang_ChestX-ray8_](http://openaccess.thecvf.com/content_cvpr_2017/html/Wang_ChestX-ray8_Hospital-Scale_Chest_CVPR_2017_paper.html)
491 [Hospital-Scale_Chest_CVPR_2017_paper.html](http://openaccess.thecvf.com/content_cvpr_2017/html/Wang_ChestX-ray8_Hospital-Scale_Chest_CVPR_2017_paper.html).
- 492 Chung-Yi Yang, Yi-Ju Pan, Yen Chou, Chia-Jung Yang, Ching-Chung Kao, Kuan-Chieh Huang, Jing-
493 Shan Chang, Hung-Chieh Chen, and Kuei-Hong Kuo. Using deep neural networks for predicting
494 age and sex in healthy adult chest radiographs. *Journal of Clinical Medicine*, 10(19):4431, 2021.
495 doi: 10.3390/jcm10194431. URL <https://doi.org/10.3390/jcm10194431>.
- 496 Sherry Yang, Ofir Nachum, Yilun Du, Jason Wei, Pieter Abbeel, and Dale Schuurmans. Foundation
497 models for decision making: Problems, methods, and opportunities. *arXiv preprint*, 2023.
- 498 H. Zhang, N. Dullerud, L. S. Kalantari, Q. Morris, Shalmali Joshi, and M. Ghassemi. An empirical
499 framework for domain generalization in clinical settings. In *ACM Conference on Health, Inference,*
500 *and Learning (CHIL)*, Virtual, 2021.
- 501 Haoran Zhang, Natalie Dullerud, Karsten Roth, Lauren Oakden-Rayner, Stephen Pfohl, and Marzyeh
502 Ghassemi. Improving the fairness of chest x-ray classifiers. In *Conference on Health, Inference,*
503 *and Learning*, pages 204–233. PMLR, 2022.
- 504 Yongshuo Zong, Yongxin Yang, and Timothy Hospedales. Medfair: Benchmarking fairness for
505 medical imaging. *arXiv preprint*, arXiv:2210.01725, 2022. URL [https://arxiv.org/abs/](https://arxiv.org/abs/2210.01725)
506 [2210.01725](https://arxiv.org/abs/2210.01725).

507 **NeurIPS Paper Checklist**

508 **1. Claims**

509 Question: Do the main claims made in the abstract and introduction accurately reflect the
510 paper's contributions and scope?

511 Answer: [\[Yes\]](#)

512 Justification: The main claims in the abstract and introduction accurately reflect the paper's
513 contributions and scope.

514 Guidelines:

- 515 • The answer NA means that the abstract and introduction do not include the claims
516 made in the paper.
- 517 • The abstract and/or introduction should clearly state the claims made, including the
518 contributions made in the paper and important assumptions and limitations. A No or
519 NA answer to this question will not be perceived well by the reviewers.
- 520 • The claims made should match theoretical and experimental results, and reflect how
521 much the results can be expected to generalize to other settings.
- 522 • It is fine to include aspirational goals as motivation as long as it is clear that these goals
523 are not attained by the paper.

524 **2. Limitations**

525 Question: Does the paper discuss the limitations of the work performed by the authors?

526 Answer: [\[Yes\]](#)

527 Justification: The paper discusses potential limitations of the work performed.

528 Guidelines:

- 529 • The answer NA means that the paper has no limitation while the answer No means that
530 the paper has limitations, but those are not discussed in the paper.
- 531 • The authors are encouraged to create a separate "Limitations" section in their paper.
- 532 • The paper should point out any strong assumptions and how robust the results are to
533 violations of these assumptions (e.g., independence assumptions, noiseless settings,
534 model well-specification, asymptotic approximations only holding locally). The authors
535 should reflect on how these assumptions might be violated in practice and what the
536 implications would be.
- 537 • The authors should reflect on the scope of the claims made, e.g., if the approach was
538 only tested on a few datasets or with a few runs. In general, empirical results often
539 depend on implicit assumptions, which should be articulated.
- 540 • The authors should reflect on the factors that influence the performance of the approach.
541 For example, a facial recognition algorithm may perform poorly when image resolution
542 is low or images are taken in low lighting. Or a speech-to-text system might not be
543 used reliably to provide closed captions for online lectures because it fails to handle
544 technical jargon.
- 545 • The authors should discuss the computational efficiency of the proposed algorithms
546 and how they scale with dataset size.
- 547 • If applicable, the authors should discuss possible limitations of their approach to
548 address problems of privacy and fairness.
- 549 • While the authors might fear that complete honesty about limitations might be used by
550 reviewers as grounds for rejection, a worse outcome might be that reviewers discover
551 limitations that aren't acknowledged in the paper. The authors should use their best
552 judgment and recognize that individual actions in favor of transparency play an impor-
553 tant role in developing norms that preserve the integrity of the community. Reviewers
554 will be specifically instructed to not penalize honesty concerning limitations.

555 **3. Theory Assumptions and Proofs**

556 Question: For each theoretical result, does the paper provide the full set of assumptions and
557 a complete (and correct) proof?

558 Answer: [\[Yes\]](#)

559 Justification: The paper includes all necessary assumptions and complete, correct proofs for
560 each theoretical result, with proper references and cross-referencing.

561 Guidelines:

- 562 • The answer NA means that the paper does not include theoretical results.
- 563 • All the theorems, formulas, and proofs in the paper should be numbered and cross-
564 referenced.
- 565 • All assumptions should be clearly stated or referenced in the statement of any theorems.
- 566 • The proofs can either appear in the main paper or the supplemental material, but if
567 they appear in the supplemental material, the authors are encouraged to provide a short
568 proof sketch to provide intuition.
- 569 • Inversely, any informal proof provided in the core of the paper should be complemented
570 by formal proofs provided in appendix or supplemental material.
- 571 • Theorems and Lemmas that the proof relies upon should be properly referenced.

572 4. Experimental Result Reproducibility

573 Question: Does the paper fully disclose all the information needed to reproduce the main ex-
574 perimental results of the paper to the extent that it affects the main claims and/or conclusions
575 of the paper (regardless of whether the code and data are provided or not)?

576 Answer: [No]

577 Justification: The paper does not fully disclose all information needed for reproducing
578 the experimental results, as the code will not be released until the paper is accepted for
579 publication at another conference. However, the dataset is openly available for use in
580 experimentation.

581 Guidelines:

- 582 • The answer NA means that the paper does not include experiments.
- 583 • If the paper includes experiments, a No answer to this question will not be perceived
584 well by the reviewers: Making the paper reproducible is important, regardless of
585 whether the code and data are provided or not.
- 586 • If the contribution is a dataset and/or model, the authors should describe the steps taken
587 to make their results reproducible or verifiable.
- 588 • Depending on the contribution, reproducibility can be accomplished in various ways.
589 For example, if the contribution is a novel architecture, describing the architecture fully
590 might suffice, or if the contribution is a specific model and empirical evaluation, it may
591 be necessary to either make it possible for others to replicate the model with the same
592 dataset, or provide access to the model. In general, releasing code and data is often
593 one good way to accomplish this, but reproducibility can also be provided via detailed
594 instructions for how to replicate the results, access to a hosted model (e.g., in the case
595 of a large language model), releasing of a model checkpoint, or other means that are
596 appropriate to the research performed.
- 597 • While NeurIPS does not require releasing code, the conference does require all submis-
598 sions to provide some reasonable avenue for reproducibility, which may depend on the
599 nature of the contribution. For example
 - 600 (a) If the contribution is primarily a new algorithm, the paper should make it clear how
601 to reproduce that algorithm.
 - 602 (b) If the contribution is primarily a new model architecture, the paper should describe
603 the architecture clearly and fully.
 - 604 (c) If the contribution is a new model (e.g., a large language model), then there should
605 either be a way to access this model for reproducing the results or a way to reproduce
606 the model (e.g., with an open-source dataset or instructions for how to construct
607 the dataset).
 - 608 (d) We recognize that reproducibility may be tricky in some cases, in which case
609 authors are welcome to describe the particular way they provide for reproducibility.
610 In the case of closed-source models, it may be that access to the model is limited in
611 some way (e.g., to registered users), but it should be possible for other researchers
612 to have some path to reproducing or verifying the results.

613
614
615
616
617
618
619
620
621
622
623
624
625
626
627
628
629
630
631
632
633
634
635
636
637
638
639
640
641
642
643
644
645
646
647
648
649
650
651
652
653
654
655
656
657
658
659
660
661
662
663
664

5. Open access to data and code

Question: Does the paper provide open access to the data and code, with sufficient instructions to faithfully reproduce the main experimental results, as described in supplemental material?

Answer: [No]

Justification: The paper does not provide open access to the code, as the code will not be released until the paper is accepted for publication at another conference. However, the dataset is openly available for experimentation.

Guidelines:

- The answer NA means that paper does not include experiments requiring code.
- Please see the NeurIPS code and data submission guidelines (<https://nips.cc/public/guides/CodeSubmissionPolicy>) for more details.
- While we encourage the release of code and data, we understand that this might not be possible, so “No” is an acceptable answer. Papers cannot be rejected simply for not including code, unless this is central to the contribution (e.g., for a new open-source benchmark).
- The instructions should contain the exact command and environment needed to run to reproduce the results. See the NeurIPS code and data submission guidelines (<https://nips.cc/public/guides/CodeSubmissionPolicy>) for more details.
- The authors should provide instructions on data access and preparation, including how to access the raw data, preprocessed data, intermediate data, and generated data, etc.
- The authors should provide scripts to reproduce all experimental results for the new proposed method and baselines. If only a subset of experiments are reproducible, they should state which ones are omitted from the script and why.
- At submission time, to preserve anonymity, the authors should release anonymized versions (if applicable).
- Providing as much information as possible in supplemental material (appended to the paper) is recommended, but including URLs to data and code is permitted.

6. Experimental Setting/Details

Question: Does the paper specify all the training and test details (e.g., data splits, hyper-parameters, how they were chosen, type of optimizer, etc.) necessary to understand the results?

Answer: [Yes]

Justification: The paper does not fully disclose all information needed for reproducing the experimental results, as the code will not be released until the paper is accepted for publication at another conference. However, the dataset is openly available for use in experimentation.

Guidelines:

- The answer NA means that the paper does not include experiments.
- The experimental setting should be presented in the core of the paper to a level of detail that is necessary to appreciate the results and make sense of them.
- The full details can be provided either with the code, in appendix, or as supplemental material.

7. Experiment Statistical Significance

Question: Does the paper report error bars suitably and correctly defined or other appropriate information about the statistical significance of the experiments?

Answer: [Yes]

Justification: The models for each experiment are trained five times with different seed numbers, and results are reported with a 95% confidence interval for robustness, with error bars appropriately included.

Guidelines:

- The answer NA means that the paper does not include experiments.

- 665
- 666
- 667
- 668
- 669
- 670
- 671
- 672
- 673
- 674
- 675
- 676
- 677
- 678
- 679
- 680
- 681
- 682
- 683
- The authors should answer "Yes" if the results are accompanied by error bars, confidence intervals, or statistical significance tests, at least for the experiments that support the main claims of the paper.
 - The factors of variability that the error bars are capturing should be clearly stated (for example, train/test split, initialization, random drawing of some parameter, or overall run with given experimental conditions).
 - The method for calculating the error bars should be explained (closed form formula, call to a library function, bootstrap, etc.)
 - The assumptions made should be given (e.g., Normally distributed errors).
 - It should be clear whether the error bar is the standard deviation or the standard error of the mean.
 - It is OK to report 1-sigma error bars, but one should state it. The authors should preferably report a 2-sigma error bar than state that they have a 96% CI, if the hypothesis of Normality of errors is not verified.
 - For asymmetric distributions, the authors should be careful not to show in tables or figures symmetric error bars that would yield results that are out of range (e.g. negative error rates).
 - If error bars are reported in tables or plots, The authors should explain in the text how they were calculated and reference the corresponding figures or tables in the text.

684 8. Experiments Compute Resources

685 Question: For each experiment, does the paper provide sufficient information on the computer resources (type of compute workers, memory, time of execution) needed to reproduce the experiments?

686 Answer: [Yes]

687 Justification: The compute resources used and run times are clearly explained in the results section.

688 Guidelines:

- 689
- 690
- 691
- The answer NA means that the paper does not include experiments.
 - The paper should indicate the type of compute workers CPU or GPU, internal cluster, or cloud provider, including relevant memory and storage.
 - The paper should provide the amount of compute required for each of the individual experimental runs as well as estimate the total compute.
 - The paper should disclose whether the full research project required more compute than the experiments reported in the paper (e.g., preliminary or failed experiments that didn't make it into the paper).

692 9. Code Of Ethics

693 Question: Does the research conducted in the paper conform, in every respect, with the NeurIPS Code of Ethics <https://neurips.cc/public/EthicsGuidelines?>

694 Answer: [Yes]

695 Justification: The research conforms to the NeurIPS Code of Ethics as it ensures informed consent, protects participant privacy, adheres to data integrity standards, and considers the societal impact of the findings.

696 Guidelines:

- 697
- 698
- 699
- The answer NA means that the authors have not reviewed the NeurIPS Code of Ethics.
 - If the authors answer No, they should explain the special circumstances that require a deviation from the Code of Ethics.
 - The authors should make sure to preserve anonymity (e.g., if there is a special consideration due to laws or regulations in their jurisdiction).

700 10. Broader Impacts

701 Question: Does the paper discuss both potential positive societal impacts and negative societal impacts of the work performed?

702 Answer: [No]

717 Justification: This research does not discuss any negative societal impacts. It is focused on
718 the performance and fairness of AI models utilizing vector-embedded chest x-ray datasets,
719 which are primarily intended for improving healthcare outcomes.

720 Guidelines:

- 721 • The answer NA means that there is no societal impact of the work performed.
- 722 • If the authors answer NA or No, they should explain why their work has no societal
723 impact or why the paper does not address societal impact.
- 724 • Examples of negative societal impacts include potential malicious or unintended uses
725 (e.g., disinformation, generating fake profiles, surveillance), fairness considerations
726 (e.g., deployment of technologies that could make decisions that unfairly impact specific
727 groups), privacy considerations, and security considerations.
- 728 • The conference expects that many papers will be foundational research and not tied
729 to particular applications, let alone deployments. However, if there is a direct path to
730 any negative applications, the authors should point it out. For example, it is legitimate
731 to point out that an improvement in the quality of generative models could be used to
732 generate deepfakes for disinformation. On the other hand, it is not needed to point out
733 that a generic algorithm for optimizing neural networks could enable people to train
734 models that generate Deepfakes faster.
- 735 • The authors should consider possible harms that could arise when the technology is
736 being used as intended and functioning correctly, harms that could arise when the
737 technology is being used as intended but gives incorrect results, and harms following
738 from (intentional or unintentional) misuse of the technology.
- 739 • If there are negative societal impacts, the authors could also discuss possible mitigation
740 strategies (e.g., gated release of models, providing defenses in addition to attacks,
741 mechanisms for monitoring misuse, mechanisms to monitor how a system learns from
742 feedback over time, improving the efficiency and accessibility of ML).

743 11. Safeguards

744 Question: Does the paper describe safeguards that have been put in place for responsible
745 release of data or models that have a high risk for misuse (e.g., pretrained language models,
746 image generators, or scraped datasets)?

747 Answer: [Yes]

748 Justification: The datasets used in this research are deidentified, which significantly reduces
749 the risk of exposing personal information. Deidentification involves removing or altering
750 identifiable information so that individuals cannot be readily identified.

751 Guidelines:

- 752 • The answer NA means that the paper poses no such risks.
- 753 • Released models that have a high risk for misuse or dual-use should be released with
754 necessary safeguards to allow for controlled use of the model, for example by requiring
755 that users adhere to usage guidelines or restrictions to access the model or implementing
756 safety filters.
- 757 • Datasets that have been scraped from the Internet could pose safety risks. The authors
758 should describe how they avoided releasing unsafe images.
- 759 • We recognize that providing effective safeguards is challenging, and many papers do
760 not require this, but we encourage authors to take this into account and make a best
761 faith effort.

762 12. Licenses for existing assets

763 Question: Are the creators or original owners of assets (e.g., code, data, models), used in
764 the paper, properly credited and are the license and terms of use explicitly mentioned and
765 properly respected?

766 Answer: [Yes]

767 Justification: The paper properly credits the creators of all assets used, explicitly mentions
768 the licenses and terms of use, and includes the relevant citations, asset versions, and URLs
769 where applicable. Each asset's license type is clearly stated, ensuring compliance with
770 copyright and terms of service.

771
772
773
774
775
776
777
778
779
780
781
782
783
784
785
786
787
788
789
790
791
792
793
794
795
796
797
798
799
800
801
802
803
804
805
806
807
808
809
810
811
812
813
814
815
816
817
818
819
820

Guidelines:

- The answer NA means that the paper does not use existing assets.
- The authors should cite the original paper that produced the code package or dataset.
- The authors should state which version of the asset is used and, if possible, include a URL.
- The name of the license (e.g., CC-BY 4.0) should be included for each asset.
- For scraped data from a particular source (e.g., website), the copyright and terms of service of that source should be provided.
- If assets are released, the license, copyright information, and terms of use in the package should be provided. For popular datasets, `paperswithcode.com/datasets` has curated licenses for some datasets. Their licensing guide can help determine the license of a dataset.
- For existing datasets that are re-packaged, both the original license and the license of the derived asset (if it has changed) should be provided.
- If this information is not available online, the authors are encouraged to reach out to the asset’s creators.

13. New Assets

Question: Are new assets introduced in the paper well documented and is the documentation provided alongside the assets?

Answer:[Yes]

Justification: The new assets introduced in the paper are well documented, with comprehensive details provided alongside the assets, including information on training, limitations, and consent processes where applicable.

Guidelines:

- The answer NA means that the paper does not release new assets.
- Researchers should communicate the details of the dataset/code/model as part of their submissions via structured templates. This includes details about training, license, limitations, etc.
- The paper should discuss whether and how consent was obtained from people whose asset is used.
- At submission time, remember to anonymize your assets (if applicable). You can either create an anonymized URL or include an anonymized zip file.

14. Crowdsourcing and Research with Human Subjects

Question: For crowdsourcing experiments and research with human subjects, does the paper include the full text of instructions given to participants and screenshots, if applicable, as well as details about compensation (if any)?

Answer:[NA]

Justification: This work does not involve with crowd sourcing and Research with Human Subjects.

Guidelines:

- The answer NA means that the paper does not involve crowdsourcing nor research with human subjects.
- Including this information in the supplemental material is fine, but if the main contribution of the paper involves human subjects, then as much detail as possible should be included in the main paper.
- According to the NeurIPS Code of Ethics, workers involved in data collection, curation, or other labor should be paid at least the minimum wage in the country of the data collector.

15. Institutional Review Board (IRB) Approvals or Equivalent for Research with Human Subjects

821
822
823
824
825
826
827
828
829
830
831
832
833
834
835
836
837
838

Question: Does the paper describe potential risks incurred by study participants, whether such risks were disclosed to the subjects, and whether Institutional Review Board (IRB) approvals (or an equivalent approval/review based on the requirements of your country or institution) were obtained?

Answer: [No]

Justification: This work does not require Institutional Review Board (IRB) approvals or equivalent review for research involving human subjects.

Guidelines:

- The answer NA means that the paper does not involve crowdsourcing nor research with human subjects.
- Depending on the country in which research is conducted, IRB approval (or equivalent) may be required for any human subjects research. If you obtained IRB approval, you should clearly state this in the paper.
- We recognize that the procedures for this may vary significantly between institutions and locations, and we expect authors to adhere to the NeurIPS Code of Ethics and the guidelines for their institution.
- For initial submissions, do not include any information that would break anonymity (if applicable), such as the institution conducting the review.